Minority Carrier Accumulation and Interfacial Kinetics in Nanosized Pt-Dotted Silicon Electrolyte Interfaces Studied by Microwave Techniques

F. Wünsch,*,† Y. Nakato,‡ and H. Tributsch†

Hahn-Meitner-Institut, Glienicker Str. 100, D-14109 Berlin, Germany, and Department of Chemistry, Graduate School of Engineering Science, Osaka University, Toyonaka, Osaka 560-8531, Japan

Received: April 19, 2002; In Final Form: August 12, 2002

Photoinduced microwave conductivity (PMC) measurement allows the determination of the excess densities of accumulating minority carriers in the potential region of the kinetically limited, increasing photocurrent. Compared with PMC signals obtained with slightly oxidized naked silicon interfaces, those for the Pt-dotted silicon interfaces have a bell shaped narrow distribution and are negatively shifted with respect to the photocurrent−potential curve. It is shown that minority carrier accumulation is essentially controlled by the peculiar Si/Pt particle interfacial barrier which can be easily overcome by holes at increasingly positive potential to take advantage of the Pt-mediated reactivity. The potential and light dependent transfer rate of minority carriers at the interface strongly increases with the applied potential. Electrochemical corrosion essentially leads to a gradual modification of this barrier through formation of a $Si-SiO_x-Pt$ structure. The influence of Fe^{2+}/Fe^{3+} concentration on the minority carrier accumulation profile as well as the photon flux dependence of the PMC signals can be explained as being due to a transport limitation phenomenon in the solution near the Pt particles.

Introduction

The combination of photoelectrochemical measurements with microwave conductivity measurements in the same experiment (microwave electrochemistry) allows (with proper calibration) a complete determination of the system with quantitative measurement of potential dependent interfacial charge-transfer rate constants, the surface recombination rate constant, minority carrier concentration at the interface, as well as the determination of various additional parameters of electrode/electrolyte interfaces.[1−3]

Silicon interfaces dotted with nanosized platinum particles have drawn attention because of their unusual photoelectrochemical and photophysical properties.[4−6] Because they produce high photovoltages and high quantum efficiencies, they have been proposed as improved interfaces for energy conversion.[7−9] Part of their behavior however remained unclear. Concerned is especially the mechanism of minority carrier transfer via the tiny platinum particles, the contribution of oxidized silicon areas around the Pt particles, and the mechanism of irreversible deterioration of photoelectrochemical properties. The purpose of this work is to contribute to the understanding of these phenomena by means of microwave−electrochemical studies.

Experimental Section

Sample Preparation. For all measurements, n-type silicon electrodes (8−12 Ω cm, $d = 500$ μm) with ⟨100⟩ oriented surface were prepared on a holder leaving a window for the microwave radiation on the rear side. The polished front of the sample was covered with small platinum dots, deposited by the following treatment: After etching in HF a solution of H_2PtCl_6 was dropped, dried and tempered at 300 °C under H_2-stream in order to reduce the H_2PtCl_6 to metallic Pt, for details see ref 10. The dots, 5−50 nm in diameter, are separated by large areas of Si, passivated by a thin oxide layer, so that most of the current is assumed to be transferred via the Pt-dots. After having removed the native oxide (40% hydrofluoric acid) from the back surface of the sample, a back contact was made with Gallium−Indium alloy, and the sample was fixed upon the holder with conductive silver epoxy.

Electrochemical Cell. The electrochemical cell was made by fixing a piece of plastic tube onto the sample (WE). The counter electrode (CE; Pt wire) and reference electrode (RE; Hg/Hg_2SO_4) were positioned in the electrolyte without shading the electrode surface. All electrodes are connected to a potentiostat, which measures the photocurrent while sweeping the potential.

Microwave Conductivity Studies. The Ka-band microwave radiation is led through a waveguide via a circulator to the rear side of the sample. Because of the conductivity change under modulated light-excitation, an AC component ΔP_r is added to the microwave power reflected from the sample back into the waveguide directed into a microwave detector by the circulator. This AC component as well as the AC component of the photocurrent depends on the potential applied between sample (WE) and CE. During the triangle voltage sweeps under potentiostatic conditions (5−20 mV/s), both values are measured simultaneously by use of lock-in-amplifiers and are recorded by computer. For details, see ref 11.

Results

Microwave conductivity measurements and photocurrent measurements are simultaneously performed with platinum dotted silicon electrodes as a function of potential. Figure 1 shows characteristic curves for three different times after beginning of the periodic potential cycling.

In the potential region where photocurrents increase toward the anodic saturation region, a bell-shaped microwave conduc-

* To whom correspondence should be addressed. E-mail: frank.wuensch@hmi.de. Fax: +49 30 80 62 24 34.
† Hahn-Meitner-Institut.
‡ Osaka University.

10.1021/jp021016+ CCC: $22.00
Published on Web 10/16/2002

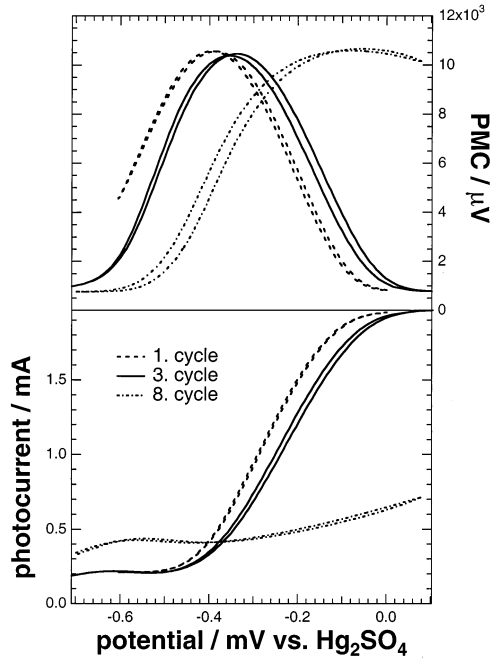

Figure 1. PMC and photocurrent vs potential for a Pt-dotted n-Si electrode (10 Ωcm, 500 μm thick, (100)) under chopped illumination at 780 nm (13.2 mWcm^{-2}) with a frequency of 827 Hz. Dashed, solid, and dash−dotted curves are for the first, third, and eighth cyclic scans, respectively. The electrolyte is 5 M HBr/0.05 M Br_2.

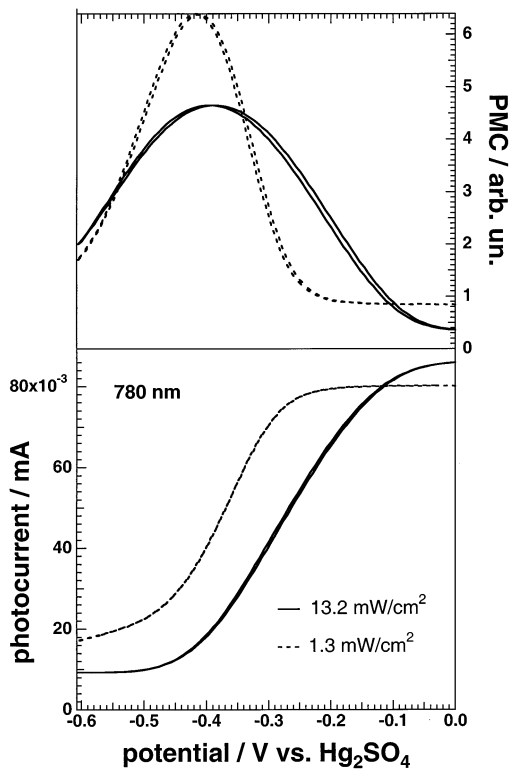

Figure 2. Illumination intensity dependence of PMC (upper half) and photocurrent (lower half) versus potential for a fresh Pt-dotted n-Si electrode. The electrolyte used is 5 M HBr/0.05 M Br_2.

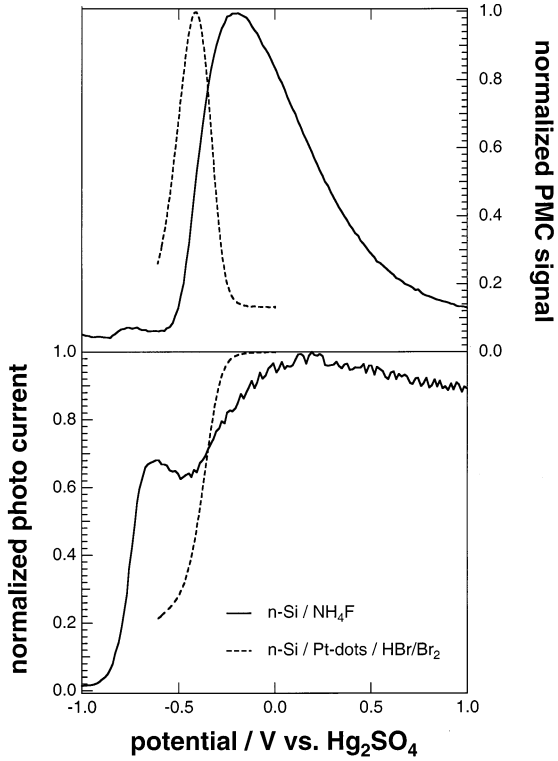

Figure 3. PMC (upper curves) and photocurrent (lower curves) for the Pt-dotted n-Si electrode in 5 M HBr/0.05 Br_2 (dashed) compared with the first forward cycle for the naked n-Si electrode in 0.1 M NH_4F (pH 0.7) after electrochemical hydrogen passivation of the surface (solid). Excitation: 780 nm, 2 mWcm^{-2}.

tivity peak is observed. It indicates that, in this potential region, minority carriers are temporarily accumulated near the electrode surface. This accumulation starts clearly before the photocurrent onset and disappears in the region where the photocurrent reaches saturation. It is important to note that the shape and position of curves of both the microwave conductivity and photocurrent signals are changing with time (first, third, and eighth cycle recorded). The maximum of the bell shaped microwave conductivity curves is shifted to the positive potential range, and they become strongly asymmetrical with time, whereas the photocurrent curve is displaced and decreases in current density in case 5 M HBr/0.05 M Br_2 is used as redox electrolyte.

Figure 2 shows how, at a fresh Pt-dotted silicon interface which is illuminated with 780 nm monochromatic light, both the width of the bell-shaped microwave conductivity curve and the onset steepness of the photocurrent change with the intensity of light. The maximum of the bell-shaped PMC curves shifts slightly toward the positive, and the width of the curves increases with increasing illumination intensity.

Pt-dotted silicon interfaces in contact with a HBr/Br_2 containing electrolyte behave distinctly different from untreated interfaces with 0.1 M NH_4F as the electrolyte. The difference is demonstrated in Figure 3, comparing the initial scan. Two remarkable changes are evident. First, the photocurrent onset occurs earlier with the Pt-dotted interface than the second photocurrent wave, which leads to photcurrent saturation. The lower potential onset for the NH_4F system is probably due to formation of OH groups as the initial (partly reversible) step[12] of an oxidation of the surface. It should therefore not be considered for the comparison of the photocurrent onsets, because it does not occur for the Pt-dotted Si surface that is already covered with a thin SiO_x layer between the Pt particles. The flatband potential can be assumed comparable (measured with microwave electrochemical techniques to be at 0.8 V for the naked silicon electrode[2,13]). This means that the surface recombination is decreased or the interfacial charge transfer rate is increased for the Pt-dotted silicon. Second, the microwave conductivity peak is sharp and close to the flatband potential

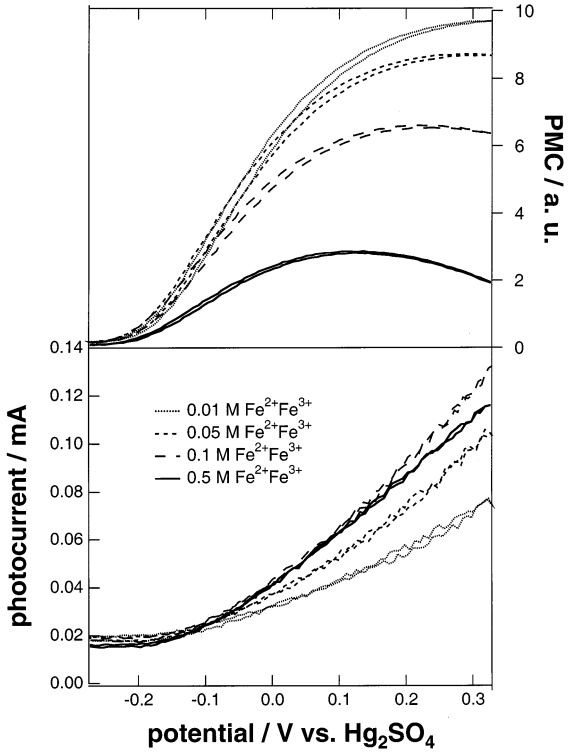

Figure 4. Dependence on the redox concentration of PMC and photocurrent vs potential for a Pt-dotted n-Si electrode in contact with a solution with Fe^{2+}/Fe^{3+} concentrations ranging from 0.01 to 0.5 M. Illumination was carried out at 660 nm (1 mW/cm^2) with a chopping frequency of 40 Hz. Inversely to the clear trend of increasing photocurrent with increasing redox concentration, the photocurrent for 0.5 M Fe^{2+}/Fe^{3+} is smaller than for 0.1 M Fe^{2+}/Fe^{3+}, because of the coloration of the solution.

for the Pt-dotted interface and is asymmetric and displaced for the naked silicon surface (with a moderately thick oxide layer). This comparison clearly suggests a distinct difference in kinetical properties of the two interfaces.

Figure 4 shows an influence of the redox-concentration with the redox potential kept unchanged. Although the photocurrent is increasing, the microwave conductivity clearly drops with increasing concentration of Fe^{2+}/Fe^{3+}. Not the redox potential but the concentration of the reduced species in the electrolyte determines consequently the accumulation of holes in the silicon interface.

Figure 5 leads back to the problem of corrosion of Pt-dotted n-Si interfaces. Although the photocurrent−potential curve shifts toward more positive potentials with repeated potential scans, the microwave conductivity peak is also shifted to the same direction (also compare Figure 1). Etching in 0.1 M HF shifts the curves again to negative potentials while changing their shape and hysteresis. Because the etching procedure removes Si-oxide, it may be concluded that the aging process increases the oxide coverage around the Pt particles.

Discussion

As shown in preceding microwave-photoelectochemical studies, the increase and subsequent decrease of microwave conductivity with increasingly positive electrode potentials is an indication for an accumulation of minority carriers at the interface. Pt-dotted silicon exhibits characteristic, bell-shaped curves, which are influenced by light intensity, the concentration of redox electrolyte, and electrochemical surface oxidation (corrosion). As previously discussed[2] the potential dependent

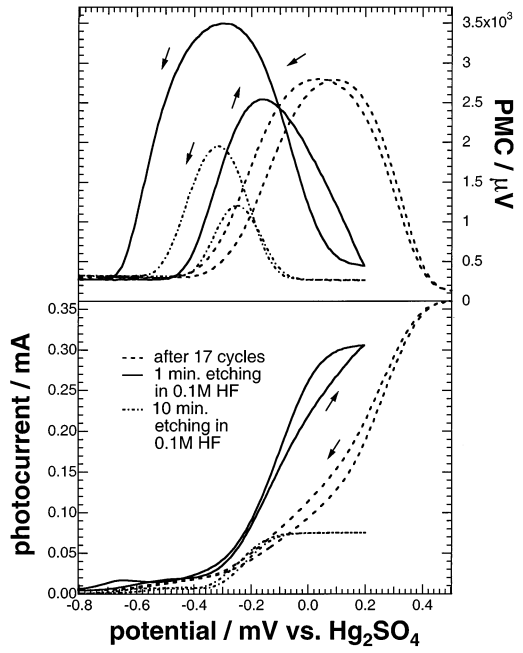

Figure 5. Degradation and recovery of PMC (upper) and photocurrent (lower) for a Pt-dotted n-Si electrode. Dotted and dashed curve are obtained after 3 and 15 cyclic scans in 5 M HBr/0.05 M Br_2 respectively, whereas solid curves are obtained with the same sample in 5 M HBr/0.05 M Br_2 after a 10 min intermediate etching in 0.1 M HF.

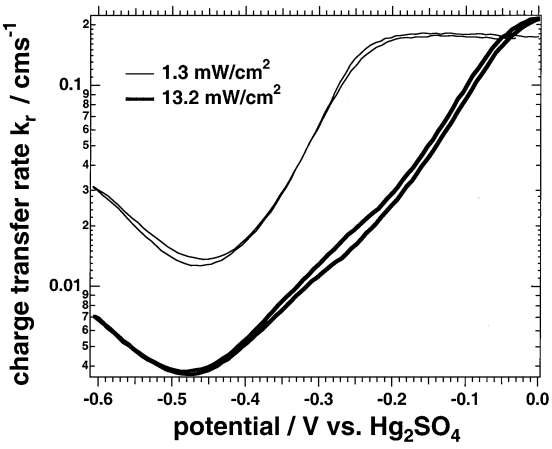

Figure 6. Charge-transfer rate k_r for minority carriers at a Pt-dotted n-Si/solution interface in a logarithmic scale as a function of electrode potential, calculated from the PMC and photocurrent data shown in Figure 2.

rate of minority carrier extraction, $k_r(\Delta U)$ can be calculated by dividing the potential dependent photocurrent Iph(ΔU) by the potential dependent PMC(ΔU) and multiplying by a known function: $\Phi(\Delta U)$, $k_r(\Delta U) \sim \mathrm{Iph}(\Delta U)\ \Phi(\Delta U)/\mathrm{PMC}(\Delta U)$. This treatment has been applied to the data of Figure 2, yielding results shown in Figure 6. It can be seen that the minority carrier collection rate $k_r(\Delta U)$ strongly increases near the onset of photocurrent (compare Figures 1 and 3) with increasing electrode potential and reaches saturation simultaneously with the saturating photocurrent. At higher light intensity, the saturation is reached at more positive electrode potential.

These observations direct attention toward the silicon−platinum particle interface which minority carriers have to cross during photoelectrochemical reactions. Figure 7 (bottom) shows schematically a cross-sectional view of the interface, and Figure 7 (top) shows the energy diagrams for a Pt particle coated

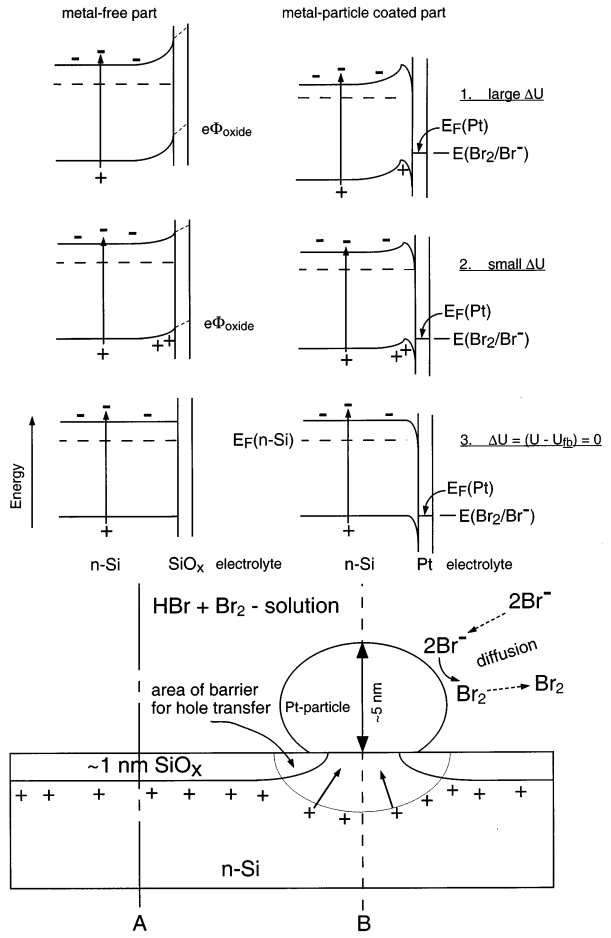

Figure 7. Schematic cross-section of the Pt-dotted n-Si/solution interface and corresponding energy diagrams. Minority carriers (holes) are accumulated near the n-Si surface at a slightly anodic bias under illumination owing to the presence of a barrier for hole transfer in the Pt-contacted interface area. Energy band diagram for explaining the accumulation of minority carriers (holes) under a small anodic bias (or small ΔU). The upper three diagrams are illustrated for the metal-free part along line (A), at different electrode potentials. The lower three diagrams are illustrating the metal−particle-coated part, along line (B). The increase in a potential drop ($\Delta\Phi_{oxide}$) in the Si-oxide layer with increasing potential (U) decreases the barrier for hole transfer to the metal.

interface (along line B) and those for a Pt-free interface (along line A) at different applied potentials. As discussed in previous papers,[4,14] because of the asymmetric electrostatic interaction of the Pt particle (∼5 nm) with the silicon, a narrow surface region with strongly negative field develops near the Pt particles (as shown in Figure 7). The minority carriers have consequently to go across or tunnel through a barrier to reach the Pt dots. When now an increasingly positive potential is applied to the Pt-dotted silicon interface, a positive space charge layer develops, leading to the accumulation of holes near the surface (Figure 7). On the other hand, the increasing space charges produce an increasing potential drop ($e\Phi_{oxide}$) in a Si-oxide layer for the Pt-free part which pushes the edge of the valence band toward increasingly positive values (Figure 7). When the positive potential is sufficiently high, minority carriers (holes) at the surface can have sufficiently large energies to go across or tunnel through and arrive on the Pt particle. When this situation is reached, the Pt particles will control the rate of reaction and no minority carrier accumulation in the silicon surface occurs. The potential dependent rate of the minority carrier collection by Pt particles (Figure 6) shows that optimum performance and potential independence is only reached at −0.2 V for an illumination of 1.3 mW/cm^2 and of 0 V for 13.2 mW/cm^2.

According to the model of Figure 7, it is expected that the Fermi level of the Pt particles shifts positively, when high intensities or low redox concentrations produce a concentration polarization near the Pt surface. This shift of the Fermi level increases the barrier for hole transfer and increases the accumulation of minority carriers as observed in experiments of Figures 2 (high light intensity) and 4. The shift in the barrier height is approximately 200 meV, when changing from a 1.3 to a 13.2 mWcm^{-2} illumination in the presence of 5 m HBr/0.05 M Br_2 containing electrolyte.

A confirmation of this model may be the observation that an increase of oxidation of the Si surface through repeated cyclic potential scans has a significant effect on the potential dependent minority carrier accumulation. An additional activation barrier appears, leading to a shift of photo current and minority carrier accumulation toward positive potentials (Figures 1 and 5). Subsequently, the oxidation process leads to a separation of platinum particles from silicon through an oxide layer (Figure 7). Finally, the electrochemical properties will degrade to a degree also observed with oxidized pure silicon surfaces (a very gradual decrease of microwave conductivity toward higher positive potentials).

Even though a more quantitative understanding of the complicated interfacial process should be attempted, the presented results demonstrate that the combination of (photo) electrochemical techniques with microwave conductivity techniques (a review is given in ref 15) permit a quite specific analysis of relevant mechanisms involved. The mechanism of (photoinduced) charge transfer can be analyzed where it is rate limited, forming a bottleneck. By studying accumulating minority carriers, it can be understood what parameters are critically involved in efficient charge transfer. Although Pt-dotted Si interfaces are already very efficient, the Pt particle/Si interface has to be optimized toward a decrease of the minority carrier accumulation and increase the carrier collection especially at low electrode potentials and at light intensities relevant for photovoltaic application.

Conclusions

This experimental study which combined electrochemical and microwave measurements essentially confirms earlier theoretical concepts on charge transfer across Pt-dot-modified silicon interfaces and quantifies the potential dependence of electron transfer rates. It shows that there still is room for optimization. To obtain a better photocurrent characteristic at solar light intensities, it may be useful to apply Pt dots of smaller dimension and more narrow size distribution (5−10 nm instead of 5−50 nm). This will lead to a minimization of the tunneling barrier.

References and Notes

(1) Schlichthörl, G.; Beck, G.; Lilie, J.; Tributsch, H. *Rev. Sci. Instrum.* **1989**, *60*, 2992.
(2) Schlichthörl, G.; Tributsch, H. *Electrochim. Acta* **1992**, *37*, 919.
(3) Schlichthörl, G.; Peter, L. M. J. *Electrochem. Soc.* **1994**, *141*, L171.
(4) Nakato, Y.; Ueda, K.; Yano, H.; Tsubomura, H. *J. Phys. Chem.* **1988**, *92*, 2316.
(5) Nakato, Y.; Ueda, K..; Tsubomura, H. *J. Phys. Chem.* **1986**, *90*, 5495.
(6) Nakato, Y.; Kai, K..; Kawabe, K. *Sol. Energy Mater. Sol. Cells* **1995**, *37*, 323.
(7) Nakato, Y.; Tsubomura, H. *Ber. Bunsen-Ges. Phys. Chem.* **1987**, *91*, 405.
(8) Nakato, Y.; Nishiura, S.; Oshika, H.; Tsubomura, H. *Jpn. J. Appl. Phys.* **1989**, *28*, L261.

(9) Jia, J.; Fujitani, M.; Yae, S.; Nakato, Y. *Electrochim. Acta* **1997**, *42*, 431.
(10) Ueda, K.; Nakato, Y.; Suzuki, N.; Tsubumura, H. *J. Electrochem. Soc.* **1989**, *136*, 2280.
(11) Wünsch, F.; Schlichthörl, G.; Tributsch, H. *J. Phys. D: Appl. Phys.* **1993**, *26*, 2041.
(12) Wünsch, F.; Nakato, Y.; Kunst, M.; Tributsch, H. *J. Chem. Soc., Faraday Trans.* **1996,** *92*, 4053.
(13) Schlichthörl, G.; Peter, L. M. *J. Electroanal. Chem.* **1995**, *381*, 55.
(14) Nakato, Y.; Tsubomura, H**.** *Electrochim. Acta* **1992**, *37*, 897.
(15) Tributsch, H. *Mod. Aspects Electrochem.* **1999**, *33*, 435.